*Manuscript
Click here to view linked References

Shape does matter: A geometric morphometric approach to shape variation in Indo-Pacific fish vertebrae for habitat identification

Sofía C. Samper Carro [a b c], Julien Louys [d], Susan O'Connor [b e]

[a] School of Archaeology and Anthropology, College of Arts and Social Sciences, Australian National University, ACT, 0200, Australia

[b] Department of Archaeology and Natural History, College of Asia and the Pacific, Australian National University, ACT, 0200, Australia

[c] Centre d'Estudis del Patrimoni Arqueològic de la Prehistoria, Facultat de Lletres, Universitat Autònoma de Barcelona

[d] Australian Research Centre of Human Evolution (ARCHE), Environmental Futures Research Institute, Griffith University, Brisbane, Australia

[e] ARC Centre of Excellence for Australian Biodiversity and Heritage, Australian National University, ACT, 0200, Australia

Abstract

Traditional fish vertebrae identification relies on the availability of comprehensive reference collections that include every element from the neural spine for each taxon. In regions with great taxonomic diversity, such as the Indo-Pacific, the identification of fish vertebrae to species is difficult. This results in taxonomic lists with many skeletal elements identified only to family. However family level identifications often tell us little about the environmental preferences of the fish and thus, by inference, human fishing practices. Here we apply geometric morphometrics (GM) to examine shape variations within vertebrae in modern specimens of a variety of pelagic and reef species to determine if this method can be used to reliably inform on habitat preferences. Digitized vertebral elements of reef (Acanthuridae, Balistidae, Labridae, Lethrinidae, Lutjanidae and Serranidae) and pelagic/open water (Scombridae and Carangidae) families were scored using 2D landmarks. These were subjected to Generalized Procrustes Analysis and discriminatory multivariate analyses (Linear Discriminant Analysis and Discriminant Function Analysis) in order to assess whether shape can be used to differentiate habitats. Our results suggest that geometric morphometrics do allow the differentiation of habitat in vertebrae and provide an alternative method for the classification of archaeological fish assemblages. These analyses were applied to a sample of archaeological fish remains from a site in Alor Island (Nusa Tenggara Timur, Indonesia) and compared with the results of an earlier traditional comparative icthyoarchaeological analysis. We found that the main component of the Pleistocene marine human diet comprised reef species, with the sporadic

addition of open water species, supporting the pattern recorded with traditional analyses. This methodology could be widely applied to archaeological fish material from across the Indo-Pacific allowing a greater number of bones in assemblages to contribute to insights into human exploitation of coastal habitats and fishing techniques over time.

Keywords: Geometric morphometrics, fish habitat, Wallacea, zooarchaeology, icthyoarchaeology, vertebrae

Introduction

Fish bones often dominate Indo-Pacific zooarchaeological assemblages. In most cases, fish vertebrae constitute the largest component of these assemblages, although until recently these elements were largely excluded from lower level taxonomic identifications (e.g. Desse and Desse, 1976; Lambrides and Weisler, 2015a, 2015b; Guillaud et al., 2016). The identification of fish vertebrae to family requires a comprehensive reference collection, with complete fish vertebral columns as well as broad species representation within families. Despite such difficulties, the importance of vertebrae when analysing archaeological fish remains is well recognised, as their inclusion increases the number of elements (NISP) and number of individuals (MNI) in an assemblage, and provides a means for estimating fish size and seasonality of capture, in both archaeological and non-archaeological studies (Gabriel et al., 2012; Granadeiro and Silva, 2000; Lambrides and Weisler, 2015a, 2016; Samper Carro, et al., 2017; Van Neer et al., 1999). Moreover, comparisons between the representation of cranial and post-cranial elements may provide insights about fish processing and fishing techniques (Butler, 1993; Zohar and Biton, 2011; Zohar and Cooke, 1997; Zohar and Dayan, 2001; Zohar et al., 2008).

Geometric morphometrics (GM), commonly used in biology to study shape variation (Zeldith, et al., 2004), has frequently been applied to the analysis of morphometric differences in *Homo* and animal species. Some examples of the application of GM include the identification of domestic traits and evolutionary history in ISEA pigs based on molar and cranial shape differences (Cucchi et al., 2009; Evin et al., 2013; Ottoni et al., 2013; Owen et al., 2014); diversity and similarities of domestic and wild canids and feeding habits based on skull shape (Drake, 2011; Drake and Klingenberg, 2010; Meloro et al., 2015); taxonomic classification of Indonesian Pleistocene cervids (Gruwier et al., 2015); and methodological and morphological analyses of bone and dental morphology on great apes and humans (Gómez-Robles et al., 2007;

Lockwood et al., 2002; Pérez et al., 2006). These methods have also been applied to non-archaeological fish remains, especially fish otoliths and scales, to assess taxonomic differences (e.g. Ponton, 2006; Ibañez, et al., 2007; Duarte, et al., 2017), or the origin of specimens in fish markets to address food safety policies (Ibañez, 2015). Recent research has also applied GM for the taxonomic identification of fish vertebrae from modern and archaeological assemblages (De Schepper et al., 2007; Guillaud et al., 2016). However, such studies have yet to examine fish habitat, a subject particularly pertinent to arguments regarding the maritime technological abilities of late Pleistocene peoples in Wallacea.

Claims of pelagic fishing ca. 42 ka cal BP at Jerimalai shelter in Timor-Leste indicated that the first humans to reach the Wallacean archipelago were already in possession of complex maritime and fishing technology and were able to carry out sustained fishing of pelagic species. This claim was based on the high proportion of Scombridae (tuna and mackerels) in the Pleistocene levels of the site (O'Connor et al. 2011). However, Anderson (2013a; 2013b) pointed out that claims for pelagic fishing at Jerimalai are problematic as the fish bones found in the Pleistocene levels were identified only as Scombridae, and as identifications were based entirely on vertebrae, sub-family, tribe, genus or species within Scombridae were not positively identified in the assemblage. As more than 22 scombrid species are currently found in the waters around Timor, and neritic tunas and mackerels outnumber oceanic tunas such as yellowfin, albacore and skipjack, Anderson (2013a) argued that the claims for both tuna fishing and pelagic fisheries in the Pleistocene at Jerimalai are unsustainable.

Here we apply GM to identify shape variation of fish vertebrae and examine to what extent shape can inform on fish preferred habitats. We evaluate how shape variations along the vertebral column could reflect differences in habitat. In doing so, we provide a benchmark for the quantitative identification of fish vertebrae. This methodology may allow more reliable identification of vertebrae based on shape, and thus a better grounding for the identification of pelagic versus in-shore fishing, with important implications for interpreting human fishing technology and behaviour from Pleistocene archaeological sites in the Indo-Pacific region. We examine fish vertebrae preserved in Tron Bon Lei, Alor, Indonesia, a late Quaternary fish-rich site, to in order to examine the presence and role of pelagic fishing at this site.

Material and methods.

Modern reference material

Modern reference material is housed in the Department of Archaeology and Natural History, College of Asia and the Pacific, at the Australian National University (ANU). For this analysis,

we selected every species available from six inshore-reef herbivore, omnivore and carnivore fish families (Acanthuridae, Balistidae (including two species in the Monacanthidae family), Labridae, Lethrinidae, Lutjanidae and Serranidae; Table 1) and two open water families (Carangidae and Scombridae; Table 2), classified according to species' environmental and biological information from FishBase (Froese and Pauly, 2017) and the California Academy of Sciences' catalog of fishes (Eschmeyer, et al., 2017). These families are some of the most commonly documented in zooarchaeological assemblages from Indonesia and Timor-Leste (O'Connor, et al., 2011; Ono and Clark, 2012; Samper Carro, et al., 2016; 2017). A total of 66 specimens representing 43 species were included in our analysis (Tables 1 and 2), comprising 666 precaudal and 1216 caudal vertebrae (including both cranial and caudal sides).

Archaeological material

The archaeological fish assemblage was recovered from Tron Bon Lei, a rock shelter located on Alor Island, Indonesia (Figure 1). Three test pits were excavated at the rock shelter in 2014, with Test Pit B yielding the largest amount of archaeological material. Three occupational phases were identified based on radiocarbon dates and stratigraphic changes, ranging from the late Holocene to the late Pleistocene (Figure 1). In addition to large quantities of cultural material, this assemblage provided thousands of fish remains (O'Connor, et al., 2017; Samper Carro, et al., 2016; 2017). Due to fragmentation and the high taxonomic diversity in the region, the icthyoarchaeological elements were identified only to family. The presence/absence of fish families was based on the identification of cranial (five paired bones and "special bones") and a few postcranial remains (Samper Carro, et al., 2017). Acanthuridae, Balistidae, Scaridae, Labridae, Lethrinidae, Lutjanidae, Serranidae and Carangidae yielded the largest number of individuals, while Scombridae presence is limited to layer 11 and 12, dated to the late Pleistocene (Table 3). The Tron Bon Lei assemblage suggested that reef/inshore families were more commonly exploited throughout the sequence, while the sporadic presence of open-water/pelagic fish families increased during the late Pleistocene (Samper Carro, et al., 2016; 2017). This trend was similar to that observed in the nearby island of Timor where, as mentioned above, the presence of Scombridae vertebrae from the lower layers of Jerimalai (dated to ca. 42 ka cal BP) suggested an emphasis on pelagic fishing in the Pleistocene (O'Connor, et al., 2011).

From the total of 27,441 fish remains identified in Tron Bon Lei, 9803 are vertebrae (Samper Carro, et al., 2017). The complete zooarchaeological assemblage was temporarily transported to ANU to conduct the taxonomical and anatomical identification of the fish remains. Due to time constraints, the taxonomical identification focused on the elements easier to identify, which for

143 vertebral remains, were limited to the 1st vertebrae of a small part of the assemblage (layers 11
144 and 12). The rest of vertebrae were classified by width into four categories to track general size
145 trends: less than 3mm; 3 to 6 mm; 6 to 10 mm; larger than 10 mm.
146
147 For this study, we selected vertebrae from the two layers where both of the families including
148 open-water/pelagic species (Carangidae and Scombridae) were documented, layer 11 (dated to
149 10,110-12,545 cal BP) and layer 12 (18,890-21,000 cal BP). Based on the five paired cranial
150 elements traditionally used and the 1st vertebrae, Serranidae (n=38), Lutjanidae (n=22), Labridae
151 (n=17), Carangidae (n=16), Lethrinidae (n=13), Balistidae (n=10) and Scombridae (n=3)
152 yielded the largest MNI in layer 11, which is the layer with a largest number of remains in the
153 whole assemblage. The same families were identified in layer 12, although the number of
154 remains is lower (Samper Carro, et al., 2017). Small vertebrae (< 3 mm and 3 to 6 mm in width)
155 are the most abundant, with vertebrae larger than 10 mm in width being more common in the
156 terminal Pleistocene layers (Samper Carro, et al., 2017). For our analysis, we did not consider
157 the smallest vertebrae (< 3 mm), and focused on complete vertebrae from the other three size
158 ranges: 3 to 6 mm width; 6 to 10 mm width; and larger than 10 mm width. A total of 81
159 precaudal and 238 archaeological caudal vertebrae (including cranial and caudal sides) were
160 thus analysed.
161
162 *Methods*
163 For each individual fish, precaudal and caudal vertebrae were selected, and the cranial and
164 caudal sides of each photographed using a Nikon D5100 camera with macro lens AF-S Micro
165 NIKKOR 60mm. Vertebrae were fixed with plasticine on a supporting platform and levelled
166 using a spirit level. The camera was systematically placed at 90^{o} angle and at 15 cm from the
167 occlusal surface of the vertebrae, focusing on the centre of the vertebral body. Photographs were
168 cropped and edited with Adobe Photoshop Lightroom CC17 and Adobe Illustrator CC17. Once
169 photos were edited, a .tps file was built for each family with tpsUtil32 version 1.74.
170
171 A total of 29 2D landmarks were placed in order to define the vertebral outline and notable
172 biological features, using tpsDig2 version 2.30 software to digitize the landmarks and scale the
173 photos. Two types of landmarks were recorded: type 1 landmarks and sliding semi-landmarks.
174 Type 1 landmarks are defined as a location where multiple discrete tissues intersect at a single
175 point, defining biological features (Baab, et al., 2012; Gruwier, et al., 2015). Our landmarks 1 to
176 9 are type 1 landmarks, with the first landmark located on the vertebral centroid and the other 8
177 landmarks located at points where the vertebral processes attach to the vertebral body (Figure
178 2). Sliding semi-landmarks permit "outlines to be combined with landmark data in one analysis,

providing a richer description of shape" (Adams, et al., 2004: 8). This method, first proposed by Bookstein (1996), consists of sliding the semi-landmark points along the outline curve of a reference specimen, until they match the positions of the corresponding points along an outline (Adams, et al., 2004). Landmarks 10 to 29 are sliding semi-landmarks (Figure 2). To record the outline, we fitted the landmarks of the vertebral body's outline on a polar grid with 20 equally-space radii created with Adobe Illustrator CC17. The polar grid was scaled to the size of the vertebrae and the central point of the grid was located in the centroid of the object, while the second radius (landmark 11) was translocated to match the location of landmark 4, placed in the contact point between the right upper vertebra process and the vertebra body (Figure 2). Hence, the polar grid has the same rotation and angle of tangent at each point along the outline for each of the vertebrae analysed.

Generalized Procrustes Analysis superimposition method (GPA, also called Generalized Least Squares, GLS) was chosen (Rohlf and Slice, 1990), which superimposes landmark configurations using least-squares estimates for translation and rotation parameters (Adams, et al., 2004; Bookstein, 1986). The morphological and statistics analyses were conducted with PAST v.3.13 (Hammer, et al., 2001), MorphoJ v.1.06d (Klingenberg, 2011) and SPSS Statistics v.24. After the GPA, in order to optimize our analysis, we conducted a linear discriminant analysis (LDA) and a linear discriminant function analysis (DFA). The application of different methods of classification has been denoted meaningful to test for differences in the results due to the statistical methods applied (Guillaud, et al., 2016). For the classification of the material from the modern reference collection, we performed a leave-one-out cross validation. As the number of variables analysed was larger than the minimum number of specimens within a group, we conducted a stepwise procedure. For the DFA, we applied Mahalanobis distance stepwise method with an F probability threshold 0.05-0.10. The percentages of correctly classified cases reported are those obtained after jack-knife procedures.

To test if differences in fish vertebrae shape can be correlated to species habitat, individuals in the reference collection were grouped according to three different environments: reef; pelagic/reef; pelagic. Fish habitat was defined according to the most habitual environment described for each species in FishBase and the Catalog of Fishes (Eschmeyer, et al., 2017; Froese and Pauly, 2017). Reef habitat species were considered as those inhabiting upper water areas, near the surface or coral beds, to a depth of 20 m (Froese and Pauly, 2017). Pelagic is defined as living and feeding in the open sea, associated with the surface or middle depths of a body of water, from 0 to 200 m depth (Froese and Pauly, 2017).

Analyses were conducted for each of the fish species from the reference material to assess the accuracy of habitat preference identification based on fish vertebral shape. Precaudal and caudal elements were analysed separately and cranial and caudal sides of each vertebrae were pooled together. We conducted three different LDAs and DFAs for each family in the reference collection: 1) considering every landmark; 2) considering only type 1 landmarks; and 3) considering only sliding semi-landmarks. Archaeological elements were classified as ungrouped cases, allowing the model defined by the reference material assigned to each habitat preference to predict archaeological elements' habitat based on their vertebral shape. This analysis produces a scatter plot of specimens along the first two canonical axes, generating the maximal and second to maximal separation between all groups, with the axes being linear combinations of the original variables and the eigenvalues indicating the amount of variation explained by the axes (Hammer, et al., 2001; Hammer and Harper, 2006). We present our results as the cross-validated percentage of correctly classified specimens, including a scatter plot of the models that yielded a higher percentage of correctly classified specimens. Shape changes are illustrated by lollipop graphs and deformation grids, with a scale factor of 0.5.

Results

Precaudal vertebrae

Percentages of well-classified elements are generally high, although lower when using LDA than DFA (Table 4). Five out of six discriminant functions (DFs) extracted for precaudal elements are significant, with the first and second DFs for each model explaining 100% of variance. The higher percentages were obtained when considering the 29 landmarks defined in precaudal elements in both LDA (71.8%) and DFA (83.6%).

Table 5 shows the habitat predicted for every precaudal vertebra, including the reference material and the archaeological assemblage. Reef category yields the higher percentages, while the differences between pelagic/reef and pelagic are less significant based on the high percentage of vertebrae classified as pelagic within the elements originally included in the pelagic/reef category. A similar result is observed for the pelagic elements, with percentages ranging from 13.7% to 32.6% for vertebral shape corresponding to the pelagic/reef predicted group.

The graphs resulting from the shape difference analyses, among the three habitat groups defined, suggest shape changes between pelagic/reef and pelagic are discrete compared to the differences observed between pelagic and reef vertebral shapes (Figure 3). Shape differences are

characterised by changes in the top and bottom half of the vertebrae, with reef vertebrae being wider on the top and narrower on the bottom compared to pelagic elements (Figure 3A). These differences are smaller and concentrated in the caudal section among pelagic/reef and reef elements (Figure 3B), while pelagic vertebrae are wider on the ventral section than pelagic/reef elements (Figure 3C). In all three mean shapes, in addition to small differences in the general outline, the larger shape changes are recorded for the landmarks defining the points where the vertebral processes attach to the vertebral body (especially, landmarks 2, 3, 5, 6, 7 and 9), with reef specimens showing wider vertebral processes and larger neural and ventral arches.

The plot of the first two DFs for the model including every landmark illustrates some degree of overlap between pelagic/reef and pelagic vertebral groups (Figure 4). The centroid of pelagic/reef and pelagic groups are separated, indicating two distinctive groups, although the morphospace regions overlap. Most of the archaeological vertebrae are plotted within the morphospace defined by the reef category.

For archaeological elements, a higher percentage of specimens are assigned to the reef category based on the models defined by every landmark and type 1 landmarks (Table 5). Sliding semi-landmarks classifies a larger number of vertebrae as pelagic/reef, while the pelagic category yields the lower percentages in all three shape models. Archaeological samples divided by context and vertebral size show a higher percentage of specimens in the 3 to 6 mm width category assigned to the reef habitat in layer 11, while the low number of precaudal vertebrae documented in layer 12 does not yield significant results (Table 6).

Caudal vertebrae

The DFA percentages obtained for habitat classification from caudal vertebrae shape are higher than the values yield by LDA in the three models tested (Table 4). The six DFs extracted are significant, with the first DF for the type 1 landmark model yielding the higher percentage of variance (Table 4; Wilk's lambda= 0.554, Chi-Square= 713.041, df= 20, p <0.0001, % variance= 95.3). However, the higher percentage of correctly classified vertebrae were obtained for the model including all landmarks, both through LDA (75.5%) and DFA (84%).

High percentages are obtained for both reef and pelagic/reef predicted groups (Table 7), while the values for pelagic-like elements are lower, especially for the type 1 landmarks' model. Differences in the percentages resulting from the comparison between pelagic/reef and pelagic

categories are higher than in the precaudal elements when considering every landmark and sliding semi-landmarks, while the differences based on type 1 landmarks are less significant.

Figure 5 includes the lollipop graphs and transformation grids between the three habitat groups, when comparing the mean shape defined in the outline including every landmark. Shape differences are more acute than in the precaudal elements, especially for the pelagic and pelagic/reef categories compared to reef specimens. Pelagic-classified vertebrae are narrower in diameter and in the top half, as illustrated by the deformed top right corner on the grid (Figure 5A). A similar difference is observed between pelagic/reef and reef elements, with additionally shape changes identified in relation to landmarks 6 and 7 (Figure 5B). Conversely, the shape comparison between pelagic and pelagic/reef vertebrae results in small shape differences, concentrated in the bottom type 1 landmarks (6 to 9; Figure 5C). In general, pelagic and pelagic/reef vertebrae yield a narrower outline in the caudal section and slightly narrower in the ventral sections, with distinctive changes in the location of the point of attachment of the vertebral processes and the vertebral body and the dimensions of the neural and hemal arches.

For the model with a higher percentage of correctly classified elements (i.e. including every landmark) the plot of the two first DFs indicate the three habitat categories are clearly distinct based on their centroids, although some overlap is observed between the morphospaces of each of the three groups (Figure 6). A large number of archaeological caudal vertebrae within the reef elements' morphospace, with fewer remains assigned to pelagic/reef and pelagic categories.

The plot in figure 6 illustrates the percentages for archaeological elements included in table 7, where archaeological caudal vertebrae assigned to the reef category yields the higher percentage (68.1%), followed by pelagic (23.1%). When separated by context and vertebral width, both layer 11 and 12 yielded a higher number of vertebrae assigned to the reef category, with the percentage for pelagic elements being higher in layer 12. The percentages for the pelagic/reef category are low in both layers.

Discussion

The application of GM to classify Indo-Pacific fish vertebrae based on habitat preference yielded high percentages of correctly classified material, expanding some of the aspects previously discussed in the analysis of vertebral shape as a taxonomical discriminant in archaeological assemblages (Guillaud, et al, 2016). As denoted by these researches, LDA percentages are lower than those obtained by other statistical methods. We selected DFA

analysis as an alternative method, as it permits the establishment of a variable range (i.e. habitat groups) that will be applied to predict the categories in which the archaeological material will be classified. DFA results yielded higher percentages, ranging from 69.8% (caudal sliding semi-landmarks) to 84% (caudal all landmarks), than LDA (63.6%-75.5%). Our results indicate that the landmark configuration that includes all the type 1 and sliding semi-landmarks provide the higher discrimination rate when analysing Indo-Pacific fish vertebrae.

An issue to consider is the classification error obtained in the modern reference material. In our best model, DFA yielded a percentage of 16% misclassified material, which may seem a high degree of uncertainty when making interpretation based on these results, as opposed to traditional identification methods. However, it is complicated to quantify the error obtained through traditional identification compared to model-based identifications. Aspects such as inter- and intra-observer reliability, incomplete reference collections and even inconsistencies in the recording of the assemblage have been suggested as sources of discrepancies in observations and measurements (e.g. Fish, 1978; Blumenschine, et al., 1996; Lyman and Van Pool, 2009). We anticipate that the addition of more modern reference species will increase the accuracy of the model, decreasing the percentage of misclassified specimens. Moreover, our method may permit the identification to habitat of more remains in an archaeological assemblage, overcoming limitations that result from incomplete reference collections and high diversity environments.

The morpho-anatomical regionalization of the vertebral column suggested for salmonids (Meunier and Ramzu, 2006), which is noted as a reason for the differences in discrimination rate between precaudal and caudal vertebrae by Guillaud and colleagues (2016), is not as marked in our study, based on the jack-knifed percentages. Including all landmarks, percentages for correctly classified precaudal (83.6%) and caudal (84%) vertebrae are similar, suggesting the complete vertebral column would be affected homogenously by morphological differences related to habitat preferences. However, the visual examination of the shape differences shows that shape variation among precaudal vertebrae are smaller compared to the mesh deformations observed for caudal vertebrae (Figures 3 and 5), especially when comparing pelagic and pelagic/reef elements with reef-dwelling species. These results suggest changes in the morphology of fish vertebrae are marked enough to distinguish between habitat groups and we anticipate that these changes are directly linked to fish locomotion.

The analysis of fish swimming mechanics, using body shape as one proxy to address fish locomotion, has a long history (Lauder, 2015). Additionally, researchers have addressed the

morpho-functionality of vertebrae in some fish species in relation to fish locomotion (Meunier and Desse, 1978; Meunier and Ramzu, 2006), which is closely correlated with fish habitat and niche. In the assemblage analysed, the main shape differences observed indicate a trend towards narrower vertebrae on pelagic and pelagic/reef specimens compared to reef-dwelling species, as well as changes in the location of type 1 landmarks, leading to narrower vertebral processes and arches in the pelagic specimens. These shape changes suggest more slender bodies in the specimens assigned to the pelagic category, which would correlate to the fusiform bodies of tuna and other open water species adapted for strong and fast swimming, characteristic of body fishing motion (Lauder, 2015). Reef-dwelling species are usually slower swimmers but adapted for short and quick burst of speed, and propelled by fin motion as in the balistiform or labriform motion examples (Videler, 1993; Lauder, 2015), which correlate with wider vertebrae and enlarged neural and hemal arches as seen in our study. Hence, the shape differences identified in our analysis correlate with the body shape and locomotion modes described for different fish families depending on their habitat preferences.

The application of GM permitted the accurate prediction of habitat preferences for over 300 precaudal and caudal archaeological vertebrae, increasing the number of remains that can be used to make interpretations about human behaviour in the Tron Bon Lei assemblage. Our shape analysis supports the previously published interpretations for Tron Bon Lei based on the analysis of cranial remains, which suggested that the main component of the marine human diet comprised reef species, with the sporadic addition of open water species in the early Holocene/late Pleistocene (Samper Carro, et al., 2016; 2017). DFAs for archaeological elements yielded percentages of over 20% pelagic-attributed specimens, with caudal vertebrae yielding slightly higher values for layer 12 than layer 11, although elements classified to reef habitat still dominated the assemblage.

Our research provides an alternative method for the classification of icthyoarchaeological assemblages, focusing on habitat instead of taxonomic identification. Habitat can be correlated to locomotion and therefore, can lead to interpretations about the fishing techniques and technologies human populations would have used to capture the different fishes. The coastal profile in the vicinity of Tron Bon Lei is steep, dropping 130 m within 1.5 km of the current coastline (Smith and Sandwell, 1997). Changes in sea level may explain the changes observed in fish families' representation through time (Samper Carro, et al, 2017). The combination of sea level, coastal topography, environmental conditions and sea surface temperature could have influenced fish availability and resulted in the adoption of varied fishing techniques by the Tron Bon Lei inhabitants during the different periods of occupation of the site. This would have led

394 to assemblages where fish with different habitat preferences were represented. During the Last
395 Glacial Maximum when the site was initially occupied, sea levels were at -130 m and the
396 coastal profile would have dropped steeply into deep waters. This may have brought pelagic
397 species closer to the shoreline making them more accessible for line fishing from the shore or
398 from boats close to the shore. During the Holocene as sea level rose, reef habitats would have
399 stabilized and reef fish became more accessible to the occupants of Tron Bon Lei.
400
401 Our study suggests that shape variation in fish vertebrae can be a useful tool for classifying
402 Indo-Pacific zooarchaeological assemblages according to habitat, providing a more robust
403 means of tackling controversial issues such as the appearance of pelagic fishing in the region,
404 and elucidating changes in fishing strategies and technology related to human behaviour. GM
405 techniques can supplement the data acquired from traditional comparative zooarchaeological
406 analyses, permitting the analysis of fish vertebrae. Likewise, the GM analyses described implies
407 fish vertebrae might be classified without the need of a vast physical reference collection, as the
408 models and datasets generated are available for researchers interested in testing their material
409 using the same methodology. Researchers can photograph and digitize landmarks on additional
410 material for inclusion in a general database for the Indo-Pacific region. Moreover, the addition
411 of more archaeological material from other Indo-Pacific archaeological sites will help to test the
412 model in different environments and address distinct research question, while improving the
413 resolution and application of these GM techniques. We anticipate the application of these GM
414 techniques to a larger assemblage of modern reference material, as well as more archaeological
415 material from Indonesia and Timor-Leste sites.
416
417 ***Conclusions***
418 Although the application of 2D GM techniques to perform fish taxonomic identification has
419 been tested previously (Guillaud et al., 2016), a similar methodology can be applied to analyse
420 fish habitat. Our study suggests this methodology can allow the classification of modern and
421 archaeological material from the Indo-Pacific with high accuracy, providing an alternative or
422 adjunct method for the classification of fish remains.
423
424 The identification of fish ecology and habitat is a key issue in Indo-Pacific icthyoarchaeological
425 assemblages as it has been related to human abilities and skills during the Holocene and
426 Pleistocene (O'Connor, et al., 2011). However, in environments with a high taxonomic
427 diversity, where the identification of vertebral elements to species is complicated, assigning
428 habitat based on fish family is problematic (Anderson, 2013). Moreover, the identification of
429 these skeletal elements through traditional methods requires extensive modern reference

collections containing complete skeletons; collections that are not available in every institution or research centre. Hence, our results provide an alternative way to assess fish habitat from vertebral elements, allowing the discrimination of pelagic versus reef fish in assemblages.

Results from the GM analysis of the fish vertebrae from Tron Bon Lei confirm and strengthen the findings from our previous conventional zooarchaeological analysis, that although in the early Holocene and Pleistocene fishing was predominantly focused on reef fish, pelagic fish were captured, and that pelagic fishing was more prevalent in the Pleistocene. The application of this method has thus allowed us to address the concerns raised by Anderson (2013a) and demonstrate that humans were engaged in pelagic fishing in Alor Island during the early Holocene and Pleistocene.

The addition of more modern reference specimens, especially for the pelagic category, will increase the accuracy of the model. Likewise, adding more archaeological assemblages will build up a benchmark for applying this methodology in the region. The methodology and dataset are available for international researchers (see linked research data), permitting the comparison of their material with the elements included in the database, and providing a global dataset to interpret human behaviour and fishing techniques.

Acknowledgments

The fieldwork for this project was funded by an ARC grant FL120100156 to O'Connor. Permission for the research was granted by the Indonesian government - RISTEK Foreign Research Permit (O'Connor 1304)/FRP/SM/V/2014. We would like to thank the landowners and villagers in Lerabain, the staff and students from Universitas Gadja Mada, Shimona Kealy, Stuart Hawkins and the Balai Arkeologi Organisation for their assistance in the field during the excavation. Sofia C. Samper Carro would like to thank colleagues from the 2015 ICAZ 18th Fish Remains Working Group Meeting held in Lisbon for comments and suggestion on preliminary communications of our results. We also acknowledge comments from two anonymous reviewers that have greatly improved this manuscript.

461 ***References***

462 Adams, D.C., Rohlf, F.J., Slice, D.E., 2004. Geometric morphometrics: ten years of progress
463 following the 'revolution'. *Italian Journal of Zoology* 71 (1), 5-16

464 Anderson, A., 2013a. The antiquity of sustained offshore fishing. *Antiquity* 87 (337), 879-885

465 Anderson, A. 2013b. Response to O'Connor and Ono, Bailey and Erlandson. *Antiquity* 87 (337),
466 892-895

467 Baab, K., Mcnulty, K., Rohlf, F., 2012. The shape of human evolution: a geometric
468 morphometrics perspective. *Evolutionary Anthropology* 21 (4), 151-165

469 Blumenschine, R.J., Marean, C.W., Capaldo, S.D., 1996. Blind-test of inter-analysts
470 correspondence and accuracy in the identification of cut marks, percussion marks, and carnivore
471 tooth marks on bone surfaces. *Journal of Archaeological Science* 23, 493-507

472 Bookstein, F.L., 1986. Size and shape spaces for landmark data in two dimensions. *Statistical*
473 *Science* 1 (2), 181-222

474 Bookstein, F.L., 1996. Landmark methods for forms without landmarks: localizing group
475 differences in outline shape. *Mathematical Methods in Biomedical Image Analysis*, 279-289

476 Butler, V.L., 1993. Natural versus cultural salmonid remains: origin of the Daller Roadcut
477 bones, Columbia River, Oregon, U.S.A. Journal of Archaeological Science 20, 1–24.

478 Butler, V.L., 1994. Fish feeding behaviour and fish capture: the case for variation in Lapita
479 fishing strategies. *Archaeology in Oceania* 29 (2), 81-90

480 Cucchi, T., Fujita, M., Dobney, K., 2009. New insights into pig taxonomy, domestication and
481 human dispersal in island South East Asia: Molar shape analysis of *Sus* remains from Niah
482 Caves, Sarawak. *International Journal of Osteoarchaeology* 19, 508–530.

483 De Schepper, N., Adriaens, D., Teugels, G.G., Devaere, S., Verraes, W., 2007. Shape variation
484 in the vertebrae of Anguilliform Clariidae (Ostariophysi: Siluriformes): a useful tool for
485 taxonomy? *Journal of Afrotropical Zoology*, 57–71.

486 Desse, G., Desse, J., 1976. Diagnostic des pièces rachidiennes des Téléostéens et des
487 Chondrichthyens. *Expansion Scientifique Française* 1–108.

488 Drake, A.G., 2011. Dispelling dog dogma: an investigation of heterochrony in dogs using 3D
489 geometric morphometric analysis of skull shape. *Evolution & Development* 13, 201–213.

490 Drake, A.G., Klingenberg, C.P., 2010. Large-scale diversification of skull shape in domestic
491 dogs: disparity and modularity. *The American Naturalist* 175, 289–301.

492 Duarte, M.R., Almeida Tubino, R., Monteiro-Neto, C., Martins, R.R.M., Vieira, F.C>, Andrade-
493 Tubino, M.F., Pereira Silva, E., 2017. Genetic and morphometric evidence that the jacks
494 (Carangidae) fished off the coast of Rio de Janeiro (Brazil) comprise four different species.
495 *Biochemical Systematics and Ecology* 71, 78-86

496 Evin, A., Cucchi, T., Cardini, A., Strand Vidarsdottir, U., Larson, G., Dobney, K., 2013. The
497 long and winding road: identifying pig domestication through molar size and shape. *Journal of*
498 *Archaeological Science* 40, 735–743.

Eschmeyer, W.N., Fricke, R., van der Laan, R. (eds.) 2017. Catalog of Fishes: Genera, Species, References(http://researcharchive.calacademy.org/research/ichthyology/catalog/fishcatmain.asp) Electronic version accessed 30 May 2017

Fish, P.,1978. Consistency in Archaeological Measurement and Classification: A Pilot Study. *American Antiquity, 43*(1), 86-89. doi:10.2307/279635

Froese, R., Pauly, D., 2017. FishBase. World Wide Web electronic publication. www.fishbase.org, version (02/2017)

Gabriel, S., Prista, N., Costa, M.J., 2012. Estimating meagre (Argyrosomus regius) size from otoliths and vertebrae. *Journal of Archaelogical Science* 39, 2859–2865.

Guillaud, E., Cornette, R., Béarez, P., 2016. Is vertebral form a valid species-specific indicator for salmonids? The discrimination rate of trout and Atlantic salmon from archaeological and modern times. *Journal of Archaeological Science* 65, 84–92.

Gómez-Robles, A., Martiñón-Torres, M., Bermúdez de Castro, J.M., Margvelashvili, A., Bastir, M., Arsuaga, J.L., Pérez-Pérez, A., Estebaranz, F., Martínez, L.M., 2007. A geometric morphometric analysis of hominin upper first molar shape. *Journal of Human Evolution* 53, 272–285.

Granadeiro, J.P., Silva, M.A., 2000. The use of otoliths and vertebrae in the identification and size-estimation of fish in predator-prey studies. *Cybium* 24, 383–393.

Gruwier, B., De Vos, J., Kovarovic, K., 2015. Exploration of the taxonomy of some Pleistocene Cervini (Mammalia, Artiodactyla, Cervidae) from Java and Sumatra (Indonesia): a geometric- and linear morphometric approach. *Quaternary Science Reviews* 119, 35–53.

Hammer, Ø., Harper, D.A.T., 2006. Paleontological Data Analysis. Blackwell

Hammer, Ø., Harper, D.A.T., Ryan, P.D., 2001. PAST: Paleontological Statistics software package for education and data analysis. *Palaeontologia Electronica* 4 (1), 9 pp.

Ibañez, A.L., 2015. Fish traceability: Guessing the origin of fish from a seafood market using fish scale shape. *Fisheries Research* 170, 82-88

Ibañez, A.L., Cowx, I.G., O´Higgins, P., 2007. Geometric morphometric analysis of fish scales for identifying genera, species, and local populations within the Mugilidae. *Canadian Journal of Fisheries and Aquatic Science* 64, 1091-1100

Klingenberg C.P., 2011. MorphoJ: an integrated software package for geometric morphometrics. *Molecular Ecology Resources* 11: 353-357.

Lambrides, A.B.J., Weisler, M.I., 2015a. Assessing protocols for identifying Pacific island archaeological fish remains: The contribution of vertebrae. *International Journal of Osteoarchaeology* 25 (6), 838-848

Lambrides, A.B.J., Weisler, M.I., 2015b. Applications of vertebral morphometrics in Pacific Island archaeological fishing studies. *Archaeology in Oceania* 50, 53–70

Lambrides, A.B.J., Weisler, M.I., 2016. Pacific islands ichtyoarchaeology: implications for the development of prehistoric fishing studies and global sustainability. *Journal of Archaeological Research* 24 (3), 275-324

Lauder, G.V., 2015. Fish locomotion: recent advances and new directions. Annual Review of Marine Science, 7: 521-545

Lockwood, C.A., Lynch, J.M., Kimbel, W.H., 2002. Quantifying temporal bone morphology of great apes and humans: an approach using geometric morphometrics. *Journal of Anatomy* 201, 447–464.

Lyman, R., and Van Pool, T., 2009. Metric Data in Archaeology: A Study of Intra-Analyst and Inter-Analyst Variation. *American Antiquity*, *74*(3), 485-504. doi:10.1017/S0002731600048721

Masse, W.B., 1986. A millenium of fishing in the Palau Islands, Micronesia. In Anderson. A (ed), *Traditional fishing the Pacific: ethnographical and archaeological papers from the 15th Pacific Science Congress, Pacific Anthropological Records* 37, 85-117

McCord, C.L., Westneat, W., 2016. Phylogenetic relationships and the evolution of BMP4 in triggerfishes and filefishes (Balistoidea). *Molecular Phylogenetics and Evolution* 94, 397-409

Meloro, C., Hudson, A., Rook, L., 2015. Feeding habits of extant and fossil canids as determined by their skull geometry. *Journal of Zoology* 295, 178–188.

Meunier, F.J., Desee, G., 1978. Interprétation histologique de la ¨métamorphose radiologique¨des vertèbres caudales du saumon (Salmo salar L.) lors de sa remontée en eau douce. Bull. Fr. Piscic. 271, 33-39. http://dx.doi.org/10.1051/kmae:1978004

Meunier, F.J., Ramzu, M.Y., 2006. In : Pale, C.R. (Ed), La régionalisation morphofonctionnelle de l'axe vertébral chez les Téléostéens en relation avec le mode de nage, vol. 5, 499-507

O'Connor, S., Ono, R., Clarkson, C., 2011. Pelagic fishing at 42,000 years ago before the present and the maritime skills of modern humans. *Science* 334, 1117-1121

O'Connor, S., Mahirta, Samper Carro, S.C., Hawkins, S., Kealy, S., Louys, J., Wood, R., 2017 Fishing in life and death: Pleistocene fish-hooks from a burial context in Alor Island, Indonesia. *Antiquity* 91 (360), 1451-1468

Ono, R., Clark, G., 2012. A 2,500-year record of marine resource use of Ulong Island, Republic of Palau. *International Journal of Osteoarchaeology* 22, 637–654.

Ottoni, C., Flink, L.G., Evin, A., Geörg, C., De Cupere, B., Van Neer, W., Bartosiewicz, L., Linderholm, A., Barnett, R., Peters, J., Decorte, R., Waelkens, M., Vanderheyden, N., Ricaut, F.., Çakirlar, C., Çevik, Ö., Hoelzel, A.R., Mashkour, M., Karimlu, A.Z.M., Seno, S.S., Daujat, J., Brock, F., Pinhasi, R., Hongo, H., Pérez Enciso, M., Rasmussen, M., Frantz, L., Megens, H.J., Crooijmans, R., Groenen, M., Arbuckle, B., Benecke, N., Vidarsdottir, U.S., Burger, J., Cucchi, T., Dobney, K., Larson, G., 2013. Pig domestication and human-mediated dispersal in Western Eurasia revealed through ancient DNA and geometric morphometrics. *Molecular Biology and Evolution* 30, 824–832.

Owen, J., Dobney, K., Evin, A., Cucchi, T., Larson, G., Vidarsdottir, U.S., 2014. The zooarchaeological application of quantifying cranial shape differences in wild boar and domestic pigs (*Sus scrofa*) using 3D geometric morphometrics. *Journal of Archaelogical Science* 43, 159–167.

582 Pérez, S.I., Bernal, V., González, P.N., 2006. Differences between sliding semi-landmarks
583 methods in geometric morphometrics, with an application to human craniofacial and dental
584 variation. *Journal of Anatomy* 208, 769–784.

585 Ponton, D., 2006. Is geometric morphometrics efficient for comparing otolith shape of different
586 fish species? *Journal of Morphology* 267, 750-757

587 Rohlf, F.J., Slice, D.E., 1990. Extensions of the Procrustes method for the optimal
588 superimposition of landmarks. *Systematic Zoology* 39, 40-59

589 Samper Carro, S.C., O'Connor, S., Louys, J., Hawkins, S., Mahirta, 2016. Human maritime
590 subsistence strategies in the Lesser Sunda Islands during the terminal Pleistocene-early
591 Holocene: New evidence from Alor, Indonesia. *Quaternary International* 416, 64–79

592 Samper Carro, S.C., Louys, J., O'Connor, S., 2017. Methodological considerations for
593 icthyoarchaeology from the Tron Bon Lei sequence, Alor, Indonesia. *Archaeological Research*
594 *in Asia* 12, 11-22

595 Smith, W.H., Sandwell, D.T., 1997. Global sea floor topography from satellite altimetry and
596 ship depth soundings. *Science* 277 (5334), 1956-1962

597 Van Neer, W., Lougas, L., Rijnsdorp, A.D., 1999. Reconstructing age distribution, season of
598 capture and growth rate of fish from archaeological sites based on otoliths and vertebrae.
599 *International Journal of Osteoarchaeology* 9, 116–130.

600 Videler, J.J., 1993. *Fish swimming*. Chapman & Hall, London, UK

601 Zelditch, M.L., Swiderski, D.L., Sheets, H.D., Fink, W.L., 2004. *Geometric Morphometrics for*
602 *Biologists: A Primer*. Elsevier Academic Press

603 Zohar, I., Biton, R., 2011. Land, lake, and fish: investigation of fish remains from Gesher Benot
604 Ya'aqov (paleo-Lake Hula). *Journal of Human Evolution* 60, 343–356.

605 Zohar, I., Cooke, R., 1997. The impact of salting and drying on fish bones: preliminary
606 observations of four marine species from Parita Bay, Panamá. *Archaeofauna: International*
607 *Journal of Archaeozoology* 6, 59–66.

608 Zohar, I., Dayan, T., 2001. Fish processing during the early Holocene: a taphonomic case study
609 from coastal Israel. *Journal of Archaeological Science* 28, 1041–1053.

610 Zohar, I., Belmaker, M., Nadel, D., Gafny, S., Goren, M., Hershkovitz, I., Dayan, T., 2008. The
611 living and the death: how do taphonomic processes modify relative abundance and skeletal
612 completeness of freshwater fish? *Palaeogeography, Palaeoclimatology, Palaeoecology* 258,
613 292–316.

614

615

616

617

618

Figures captions

Figure 1: Location of Alor in the Wallacean archipelago and detail of Alor island location in relation to Timor Leste, indicating Jerimalai and Lene Hara caves location (top left); Location of Tron Bon Lei in Alor island, showing the coast line during the late Pleistocene (bottom left); Archaeological sequence and chronology of Test Pit B from Tron Bon Lei (right)

Figure 2: Graphic representation of the type 1 landmarks and sliding semi-landmarks considered in this analysis

Figure 3: Lollipop graphs and transformation grids illustrating the shape differences in precaudal vertebrae documented between habitat groups in the model including all landmarks. A) reef compared to pelagic; B) reef compared to pelagic/reef; C) pelagic/reef compared to pelagic

Figure 4: Plot of the first two linear discriminant functions extracted from all landmarks values used to classify habitat within precaudal vertebrae

Figure 5: Lollipop graphs and transformation grids illustrating the shape differences in caudal vertebrae documented between habitat groups in the model including all landmarks. A) reef compared to pelagic; B) reef compared to pelagic/reef; C) pelagic/reef compared to pelagic

Figure 6: Plot of the first two linear discriminant functions extracted from all landmarks values used to classify habitat within caudal vertebrae

Tables captions

Table 1: Herbivore, omnivore and carnivore in shore/reef species used in our analysis. Ref. no.= reference number given in the ANH reference collection; LN= Total length; SL=Standard Length; Max length= Maximum length recorded from FishBase website (Froese, R. and Pauly, D., 2017)

Table 2: Species from fish families Carangidae and Scombridae used in our analysis, including the habitat preference attributed to each species. Ref. no.= reference number given in the ANH reference collection; LN= Total length; SL=Standard Length; Max length= Maximum length recorded from FishBase website (Froese, R. and Pauly, D., 2017)

Table 3: NISP by fish family documented in each of the occupation phases documented in Tron Bon Lei for the five paired cranial elements and the 1st vertebrae. Vertebrae identification was only conducted in layer 11 and 12. Phase I: 3,000-4,000 cal BP; Phase II: ca. 7,500-12,500 cal BP; Phase III: 18,890-21,000 cal BP (See figure 1 for exact dates and correlation with the archaeological sequence)

Table 4: Basic statistics for the discriminant function used for each fish family in the reference collection considering the three landmarks configurations included in the analysis, including the percentage of correctly classified elements through DFA and LDA

Table 5: Number of precaudal vertebrae classified to each habitat group through DFA and percentage of the row total for the modern reference material and archaeological elements in each of the landmark configurations tested

Table 6: Number of precaudal vertebrae classified to each habitat group through DFA and percentage of the total by layer for the archaeological elements from Tron Bon Lei

Table 7: Number of caudal vertebrae classified to each habitat group through DFA and percentage of the row total for the modern reference material and archaeological elements in each of the landmark configurations tested

Table 8: Number of caudal vertebrae classified to each habitat group through DFA and percentage of the total by layer for the archaeological elements from Tron Bon Lei

Linked research data captions

Precaudal all families and archaeological: .dat file with the raw data (landmark coordinates) including all the precaudal vertebrae analysed. Family= fish family or archaeological site; Habitat= archaeological material defined as "archaeological"; Species= the numbers refers to the catalogue number in the ANH reference collection (see tables 1 and 2) and the layer of provenance for the archaeological material; Vtb side= vertebral side (caudal or cranial) analysed; Vtb no= vertebra position in the vertebral colums or size range for the archaeological material

Caudal all families and archaeological: .dat file with the raw data (landmark coordinates) including all the caudal vertebrae analysed. Family= fish family or archaeological site; Habitat= archaeological material defined as "archaeological"; Species= the numbers refers to the catalogue number in the ANH reference collection (see tables 1 and 2) and the layer of provenance for the archaeological material; Vtb side= vertebral side (caudal or cranial) analysed; Vtb no= vertebra position in the vertebral colums or size range for the archaeological material

Table 1

Family	Scientific name	Common name	LN Total length (mm)	SL Standard length (mm)	Weight (g)	Max length (mm)
Acanthuridae	*Naso vlamingii*	Bignose unicornfish	280	-	-	600 LN
Acanthuridae	*Naso thynnoides*	Oneknife unicornfish	400	-	-	400 LN (common 250 LN)
Acanthuridae	*Naso unicornis*	Bluespine unicornfish	320	265	-	700 LN (common 500 LN)
Acanthuridae	*Acanthurus xanthopterus*	Yellowfin surgeonfish	200	160	-	700 LN (common 500 LN)
Acanthuridae	*Acanthurus* sp.	Surgeonfish	240	190	-	-
Balistidae	*Balistapus undulatus*	Orange-lined triggerfish	125	-	-	300 LN (common 260 LN)
Balistidae	*Balistapus undulatus*	Orange-lined triggerfish	215	-	-	300 LN (common 260 LN)
Balistidae	*Balistoides conspicillum*	Clown triggerfish	240	-	-	500 LN
(Monacanthidae)	*Acanthaluteres vittiger*	Toothbrush leatherjacket	240	203	150	350 LN
(Monacanthidae)	*Monacanthus* sp.	Leatherjacket	-	-	-	-
Labridae	*Bodianus loxozonus*	Blackfin hogfish	420	370		470 LN
Labridae	*Choerodon anchorago*	Orange-dotted tuskfish	-	-	-	500 LN
Labridae	*Achoerodus gouldii*	Western blue groper	290	250	412	1750 LN
Labridae	*Notolabrus gymnogenis*	Crimsonband wrasse	160	135	60	230 SL (200 SL female)
Labridae	*Notolabrus tetricus*	Blue-throated wrasse	210	185	190	500 LN
Labridae	*Notolabrus tetricus*	Blue-throated wrasse	280	240	-	500 LN
Labridae	*Notolabrus tetricus*	Blue-throated wrasse	380	330	-	500 LN
Labridae	*Notolabrus fucicola*	Yellow-saddled wrasse	255	230	230	380 LN
Labridae	*Notolabrus fucicola*	Yellow-saddled wrasse	327	290	-	380 LN
Labridae	*Cheilinus chlorourus*	Floral wrasse	160	135	-	450 LN
Labridae	*Cheilinus undulatus*	Humphead wrasse	375	335	-	2290 SL (common 600 LN)
Labridae	*Cheilinus undulatus*	Humphead wrasse	490	420	-	2290 SL (common 600 LN)
Labridae	*Cheilio inermis*	Cigar wrasse	320	285	-	500 SL (common 350 LN)
Labridae	*Cheilio inermis*	Cigar wrasse	195	170	-	500 SL (common 350 LN)
Lethrinidae	*Lethrinus semicinctus*	Black blotch emperor	590	-	3000	350 LN (common 290 SL)
Lethrinidae	*Lethrinus erythracanthus*	Orange-spotted emperor	320	-	-	700 LN (common 500 LN)
Lethrinidae	*Lethrinus amboinensis*	Ambon emperor	-	-	-	700 LN (common 400 LN)
Lethrinidae	*Lethrinus variegatus*	Slender emperor	160	130	57	200 LN
Lethrinidae	*Lethinus nebulosus*	Spangled emperor	210	175	-	870 LN (common 700 LN)

Family	Scientific name	Common name	Ref.no.	LN (mm)	SL (mm)	Weight (g)	Max length (mm)	Habitat
Lethrinidae	*Lethrinus mahsena*	Sky emperor		285	240	-	650 LN (common 400 LN)	
Lethrinidae	*Lethrinus obsoletus*	Orange-striped emperor		220	185	-	600 LN (common 300 LN)	
Lutjanidae	*Lutjanus bohar*	Two-spot red snapper		610	-	500	900 LN (common 760 LN)	
Lutjanidae	*Lutjanus rivulatus*	Blubberlip snapper		380	-	-	800 LN (common 600 LN)	
Lutjanidae	*Paracaesio kusakarii*	Saddle-back snapper		575	495		600 SL	
Lutjanidae	*Lutjanus timorensis*	Timor snapper		420	360	1000	500 LN (common 300 LN)	
Lutjanidae	*Pristipomoides argyrogrammicus*	Ornate jobfish		285	-	-	400 LN (common 250 LN)	
Serranidae	*Epinephelus fasciatus*	Blacktip grouper		150	-	-	400 LN (common 220 LN)	
Serranidae	*Cephalopholis argus*	Peacock hind		300	-	-	600 LN (common 400 LN)	
Serranidae	*Epinephelus retouti*	Red-tipped grouper		400	340	-	500 LN (common 300 LN)	
Serranidae	*Saloptia powelli*	Golden grouper		500	420	-	390 SL	
Serranidae	*Epinephelus morrhua*	Comet grouper		500	430	1000	900 LN (common 600 LN)	
Serranidae	*Cephalopholis argus*	Peacock hind		475	410	-	600 LN (common 400 LN)	

Acanthuridae	*Naso vlamingii*	Bignose unicornfish	F0174	280	-	-	600 LN	Marine reef
Acanthuridae	*Naso thynnoides*	Oneknife unicornfish	F0166	400	-	-	400 LN (common 250 LN)	Marine reef
Acanthuridae	*Naso unicornis*	Bluespine unicornfish	F0323	320	265	-	700 LN (common 500 LN)	Marine reef
Acanthuridae	*Acanthurus xanthopterus*	Yellowfin surgeonfish	F0356	200	160	-	700 LN (common 500 LN)	Marine reef
Acanthuridae	*Acanthurus* sp.	Surgeonfish	F0471	240	190	-	-	Marine reef
Balistidae	*Balistapus undulatus*	Orange-lined triggerfish	F0120	125	-	-	300 LN (common 260 LN)	Marine reef
Balistidae	*Balistapus undulatus*	Orange-lined triggerfish	F0132	215	-	-	300 LN (common 260 LN)	Marine reef
Balistidae	*Balistoides conspicillum*	Clown triggerfish	F0178	240	-	-	500 LN	Marine reef
Labridae	*Bodianus loxozonus*	Blackfin hogfish	F0371	420	370	-	470 LN	Marine reef
Labridae	*Choerodon anchorago*	Orange-dotted tuskfish	F0189	-	-	-	500 LN	Marine reef
Labridae	*Achoerodus gouldii*	Western blue groper	F0226	290	250	412	1750 LN	Marine reef
Labridae	*Notolabrus gymnogenis*	Crimsonband wrasse	F0236	160	135	60	230 SL (200 SL female)	Marine reef
Labridae	*Notolabrus tetricus*[1]	Blue-throated wrasse	F0273	210	185	190	500 LN	Marine reef
Labridae	*Notolabrus tetricus*[2]	Blue-throated wrasse	F0412	280	240	-	500 LN	Marine reef
Labridae	*Notolabrus tetricus*[3]	Blue-throated wrasse	F0424	380	330	-	500 LN	Marine reef
Labridae	*Notolabrus fucicola*	Yellow-saddled wrasse	F0278	255	230	230	380 LN	Marine reef
Labridae	*Notolabrus fucicola*	Yellow-saddled wrasse	F0382	327	290	-	380 LN	Marine reef
Labridae	*Cheilinus chlorourus*	Floral wrasse	F0347	160	135	-	450 LN	Marine reef
Labridae	*Cheilinus undulatus*	Humphead wrasse	F0348	375	335	-	2290 SL (common 600 LN)	Marine reef
Labridae	*Cheilinus undulatus*	Humphead wrasse	F0369	490	420	-	2290 SL (common 600 LN)	Marine reef
Labridae	*Cheilio inermis*	Cigar wrasse	F0349	320	285	-	500 SL (common 350 LN)	Marine reef
Labridae	*Cheilio inermis*	Cigar wrasse	F0350	195	170	-	500 SL (common 350 LN)	Marine reef
Lethrinidae	*Lethrinus semicinctus*	Black blotch emperor	F0115	590	-	3000	350 LN (common 290 SL)	Marine reef
Lethrinidae	*Lethrinus erythracanthus*	Orange-spotted emperor	F0184	320	-	-	700 LN (common 500 LN)	Marine reef
Lethrinidae	*Lethrinus amboinensis*	Ambon emperor	F0324	-	-	-	700 LN (common 400 LN)	Marine reef
Lethrinidae	*Lethrinus variegatus*	Slender emperor	F0336	160	130	57	200 LN	Marine reef
Lethrinidae	*Lethinus nebulosus*	Spangled emperor	F0340	210	175	-	870 LN (common 700 LN)	Marine reef
Lethrinidae	*Lethrinus mahsena*	Sky emperor	F0354	285	240	-	650 LN (common 400 LN)	Marine reef
Lethrinidae	*Lethrinus obsoletus*	Orange-striped emperor	F0368	220	185	-	600 LN (common 300 LN)	Marine reef

Table 2

Family	Scientific name	Common name	LN Total length (mm)	SL Standard length (mm)	Weight (g)	Max length (mm)	Habitat
Carangidae	*Pseudocaranx dentex*	White trevally	750	-	4500	1220 LN (common 400 LN)	Reef
Carangidae	*Selar crumenophthalmus*	Bigeyed scad	225	-	-	700 LN	Reef
Carangidae	*Elagatis bipinnulata*	Rainbow runner	-	-	-	1800 LN (common 900 LN)	Pelagic/reef
Carangidae	*Caranx ignobilis*	Giant trevally	650	-	4200	1700 LN (common 1000 LN)	Pelagic
Carangidae	*Elagatis bipinnulata*	Rainbow runner	-	-	-	1800 LN (common 900 LN)	Pelagic/reef
Carangidae	*Caranx lugubris*	Black jack	400	-	-	1000 LN (common 700 LN)	Pelagic
Carangidae	*Caranx lugubris*	Black jack	655	580	-	1000 LN (common 700 LN)	Pelagic
Carangidae	*Scomberoides lysan*	Doublespotted queenfish	225	250	80	1100 LN (common 600 LN)	Pelagic/reef
Carangidae	*Scomberoides lysan*	Doublespotted queenfish	-	-	-	1100 LN (common 600 LN)	Pelagic/reef
Carangidae	*Selar crumenophthalmus*	Bigeyed scad	325	280	-	700 LN	Pelagic
Carangidae	*Seriola lalandi*	Yellowtail amberjack	-	-	-	2500 LN (common 800 LN)	Pelagic
Scombridae	*Gymnosarda unicolor*	Dogtooth tuna	730	-	5750	2480 LN (common 1900 LN)	Pelagic
Scombridae	*Rastrelliger kanagurta*	Indian mackerel	320	-	-	4210 LN (common 250 LN)	Pelagic
Scombridae	*Acanthocybium solandri*	Wahoo	-	-	-	2500 LN (common 1700 LN)	Pelagic

Table 3

		Acanthuridae	Balistidae	Belonidae	Carangidae	Holocentridae	Labridae	Lethrinidae	Lutjanidae	Scaridae	Scombridae	Serranidae
Maxilla	**Phase I**	-	-	-	-	-	-	-	-	-	-	-
	Phase II	-	2	-	2	3	4	10	10	3	-	41
	Phase III	-	-	-	-	-	5	1	1	-	-	7
Premaxilla	**Phase I**	-	1	-	-	-	-	-	-	-	-	2
	Phase II	2	13	-	5	6	16	7	24	2	2	145
	Phase III	1	2	-	1	-	2	5	-	1	14	-
Dentary	**Phase I**	-	-	-	-	-	-	3	-	-	-	-
	Phase II	1	9	-	-	3	29	9	17	6	2	119
	Phase III	-	-	-	-	-	4	-	-	-	-	15
Quadrate	**Phase I**	-	-	-	1	-	-	1	-	-	-	-
	Phase II	1	29	2	7	7	4	8	15	4	3	61
	Phase III	-	6	-	-	-	-	-	4	-	-	7
Angular	**Phase I**	-	-	-	-	-	-	-	-	-	-	-
	Phase II	-	1	-	3	-	3	1	8	4	3	27
	Phase III	-	-	-	1	-	-	-	-	-	-	-
1st Vertebrae	**Phase I**	-	-	-	-	-	-	-	-	-	-	-
	Phase II (layer 11)	4	10	-	16	-	3	13	22	-	-	27
	Phase III (layer 12)	1	3	-	1	-	-	-	-	-	1	1
		10	76	2	37	19	70	58	101	20	25	452

Table 4

	Function	Wilks's lambda	Chi-Square	df	p	Eigenvalue	%of variance	Canonical correlation	%correctly classified cross-validated	LDA jackknifed
Precaudal all landmarks	DF1	0.459	510.991	30	<0.0001	1.108	92.7	0.71	83.6%	71.8%
	DF2	0.926	50.431	14	<0.0001	0.08	7.3	0.272		
Caudal all landmarks	DF1	0.474	897.035	46	<0.0001	0.875	87.5	0.683	84.0%	75.5%
	DF2	0.889	141.69	22	<0.0001	0.125	12.5	0.333		
Precaudal type 1 LM	DF1	0.535	412.997	16	<0.0001	0.839	98	0.675	81.2%	68.7%
	DF2	0.983	11.276	7	0.127	0.017	2	0.13		
Caudal type 1 LM	DF1	0.554	713.041	20	<0.0001	0.741	95.3	0.652	79.9%	69.7%
	DF2	0.965	43.108	9	<0.0001	0.036	4.7	0.187		
Precaudal semi LM	DF1	0.636	297.13	28	<0.0001	0.476	87.9	0.568	72.4%	63.6%
	DF2	0.938	41.746	13	<0.0001	0.066	12.1	0.248		
Caudal semi LM	DF1	0.667	487.062	36	<0.0001	0.37	79.8	0.52	69.8%	63.8%
	DF2	0.914	107.821	17	<0.0001	0.094	20.2	0.293		

Table 5

		Precaudal			
		Predicted group			
		Reef	Pelagic/reef	Pelagic	Total
All landmarks	Reef	467 (86%)	40 (7.4%)	36 (6.6%)	543
	Pelagic/reef	3 (10.7%)	18 (64.3%)	7 (25%)	28
	Pelagic	10 (10.5%)	13 (13.7%)	72 (75.8%)	95
	Archaeological	42 (51.9%)	22 (27.2%)	17 (21%)	81
Type 1 landmarks	Reef	469 (86.4%)	48 (8.8%)	26 (4.8%)	543
	Pelagic/reef	3 (10.7%)	15 (60.7%)	10 (28.6%)	28
	Pelagic	7 (7.4%)	31 (32.6%)	57 (60%)	95
	Archaeological	46 (56.8%)	24 (29.6%)	11 (13.6%)	81
Sliding semi-landmarks	Reef	392 (72.2%)	69 (12.7%)	82 (15.1%)	543
	Pelagic/reef	4 (14.3%)	19 (67.9%)	5 (17.9%)	28
	Pelagic	8 (8.4%)	16 (16.8%)	71 (74.7%)	95
	Archaeological	27 (33.3%)	36 (44.4%)	18 (22.2%)	81

Table 6

		Precaudal all landmarks			
		Predicted habitat			Grand Total
Context	**Size (mm)**	**Reef**	**Pelagic/reef**	**Pelagic**	
Layer 11	3-6	30 (38.5%)	10 (12.8%)	6 (7.7%)	**46 (56.8%)**
	6-10	9 (11.5%)	9 (11.5%)	7 (9%)	**25 (30.9%)**
	10	1 (1.3%)	3 (3.8%)	3 (3.8%)	**7 (8.6%)**
Layer 11 Total		**40 (51.3%)**	**22 (28.2%)**	**16 (20.5%)**	**78 (96.3%)**
Layer 12	3-6	2 (66.7%)	-	1(33.3%)	**3 (3.7%)**

Table 7

		Caudal			
		Predicted group			
		Reef	Pelagic/reef	Pelagic	Total
All landmarks	Reef	855 (86.7%)	53 (5.4%)	78 (7.9%)	986
	Pelagic/reef	0	41 (89.1%)	5 (10.9%)	46
	Pelagic	32 (17.4%)	26 (14.1%)	126 (68.5%)	184
	Archaeological	162 (68.1%)	21 (8.8%)	55 (23.1%)	238
Type 1 landmarks	Reef	844 (85.6%)	53 (5.4%)	89 (9%)	986
	Pelagic/reef	0	31 (67.4%)	15 (32.6%)	46
	Pelagic	35 (19%)	53 (28.8%)	96 (52.2%)	184
	Archaeological	143 (60.1%)	36 (15.1%)	59 (24.8%)	238
Sliding semi-landmarks	Reef	701 (71.1%)	102 (10.3%)	183 (18.6%)	986
	Pelagic/reef	2 (4.3%)	36 (78.3%)	8 (17.4%)	46
	Pelagic	39 (21.2%)	33 (17.9%)	112 (60.9%)	184
	Archaeological	108 (45.4%)	45 (18.9%)	85 (35.7%)	238

Table 8

Caudal all landmarks

		Predicted habitat			
Context	**Size**	**Reef**	**Pelagic/reef**	**Pelagic**	**Grand Total**
Layer 11	3-6	78 (47.6%)	3 (1.8%)	18 (11%)	**99 (41.6%)**
	6-10	35 (21.4%)	10 (6.1%)	14 (8.5%)	**59 (24.8%)**
	10	2 (1.2%)	2 (1.2%)	2 (1.2%)	**6 (2.5%)**
Layer 11 Total		**115 (70.1%)**	**15 (9.1%)**	**34 (20.7%)**	**164 (68.9%)**
Layer 12	3-6	43 (58.1%)	4 (5.4%)	20 (27.1%)	**67 (28.2%)**
	6-10	1 (1.4%)	-	-	**1 (0.4%)**
	10	3 (4.1%)	2 (2.7%)	1 (1.4%)	**6 (2.5%)**
Layer 12 Total		**47 (63.5%)**	**6 (8.1%)**	**21 (28.4%)**	**74 (31.1%)**

Figure 1

Click here to download high resolution image

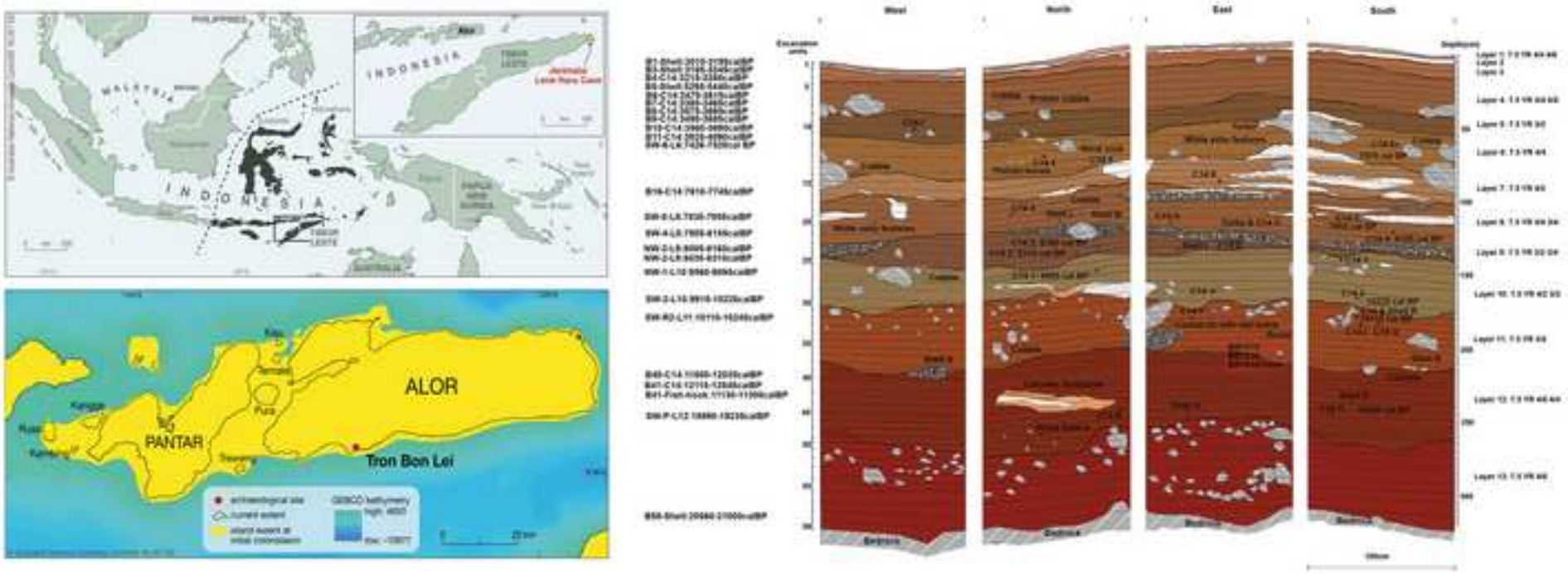

Figure 2

Click here to download high resolution image

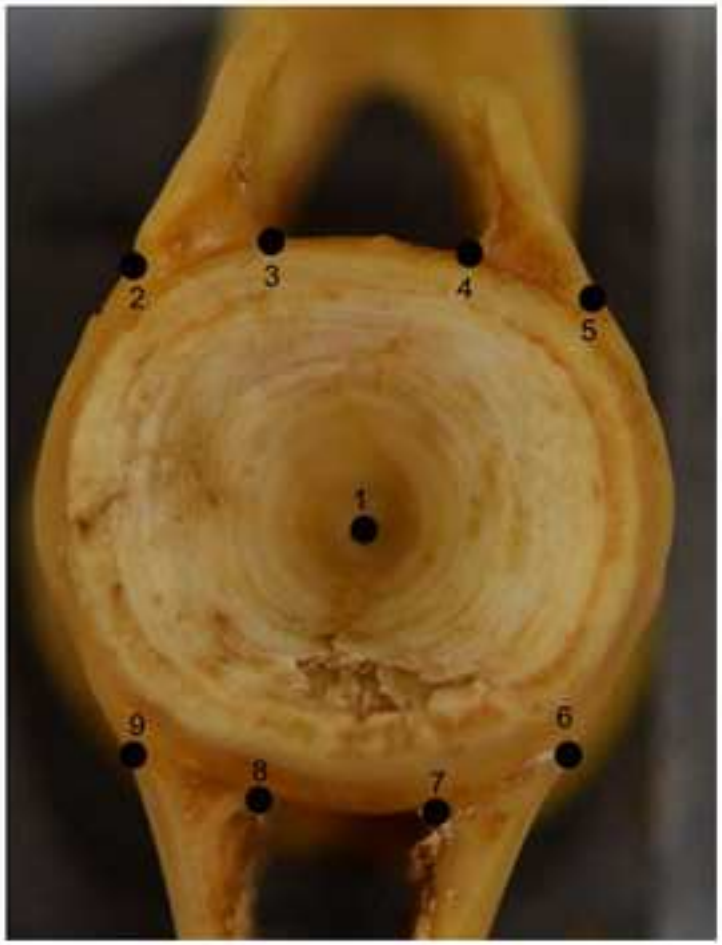

Type 1 landmarks

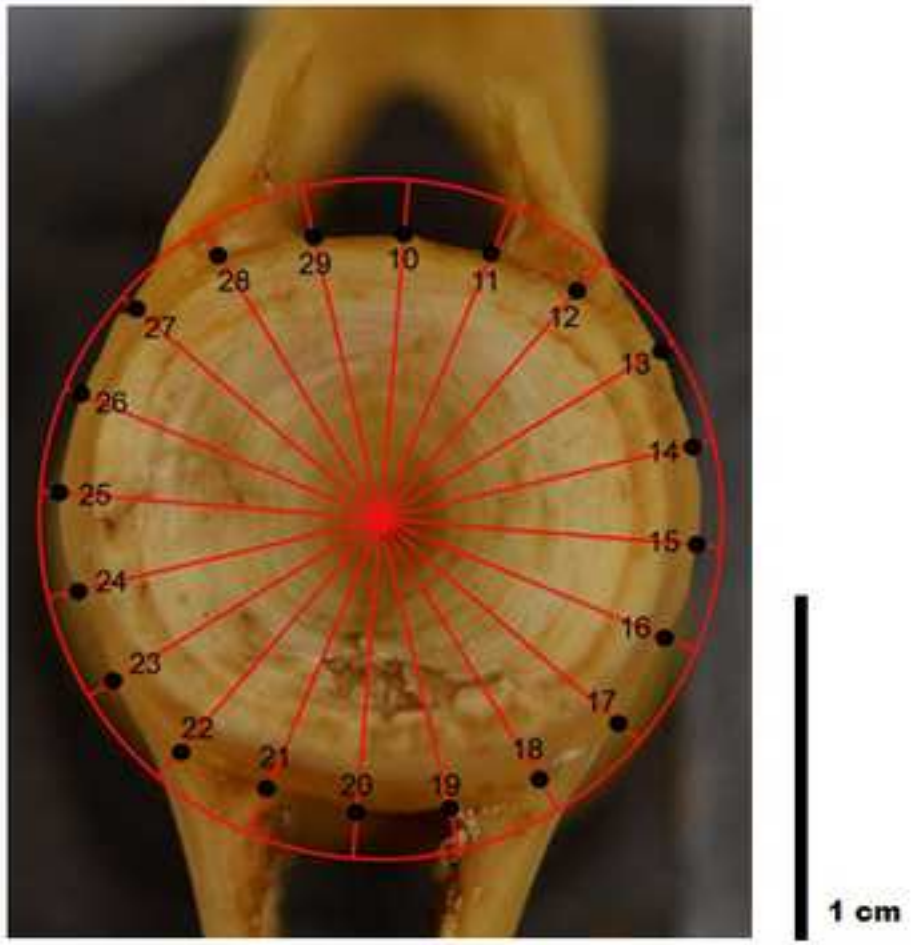

Sliding semi-landmarks

Figure 3

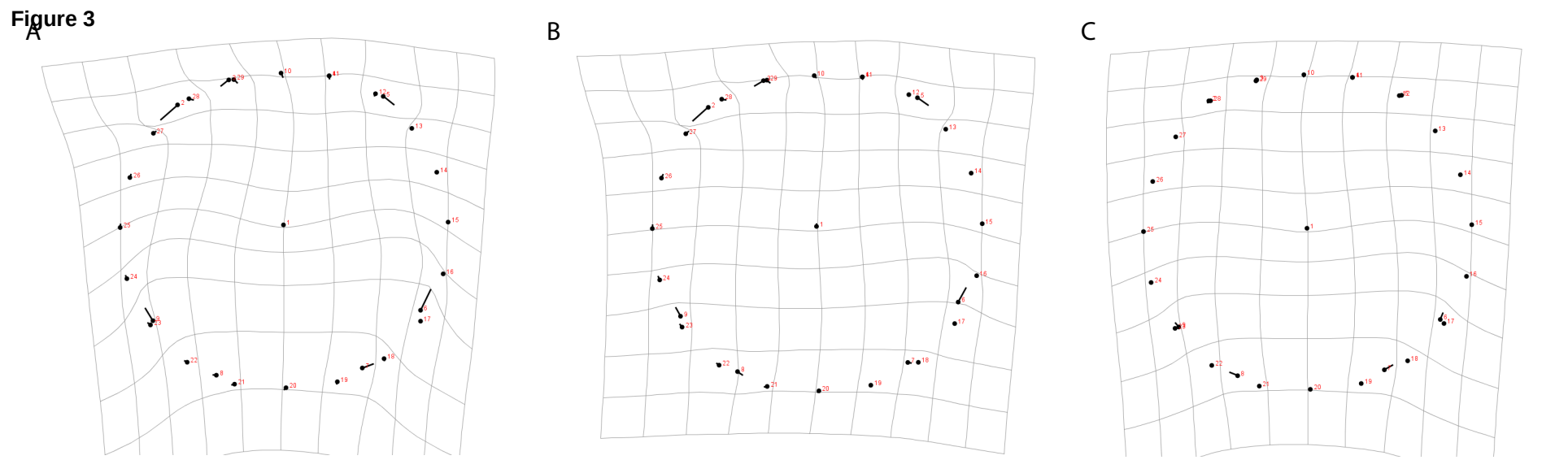

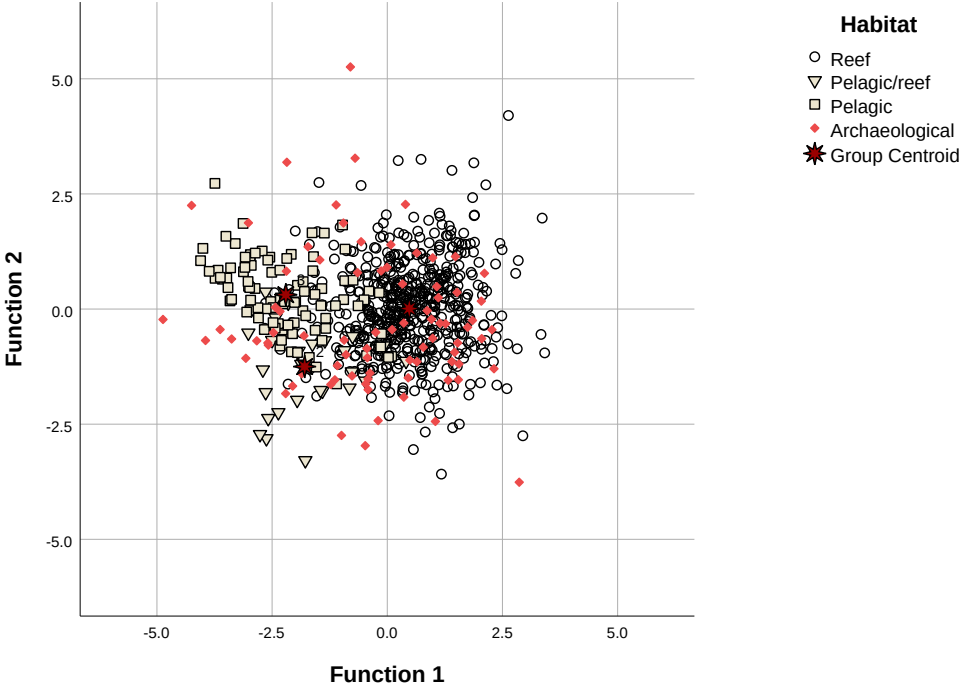
Habitat
Reef
Pelagic/reef
Pelagic
Archaeological
Group Centroid
Function 2
5.0
2.5
0.0
-2.5
-5.0
Function 1
-5.0
-2.5
0.0
2.5
5.0

Figure 5

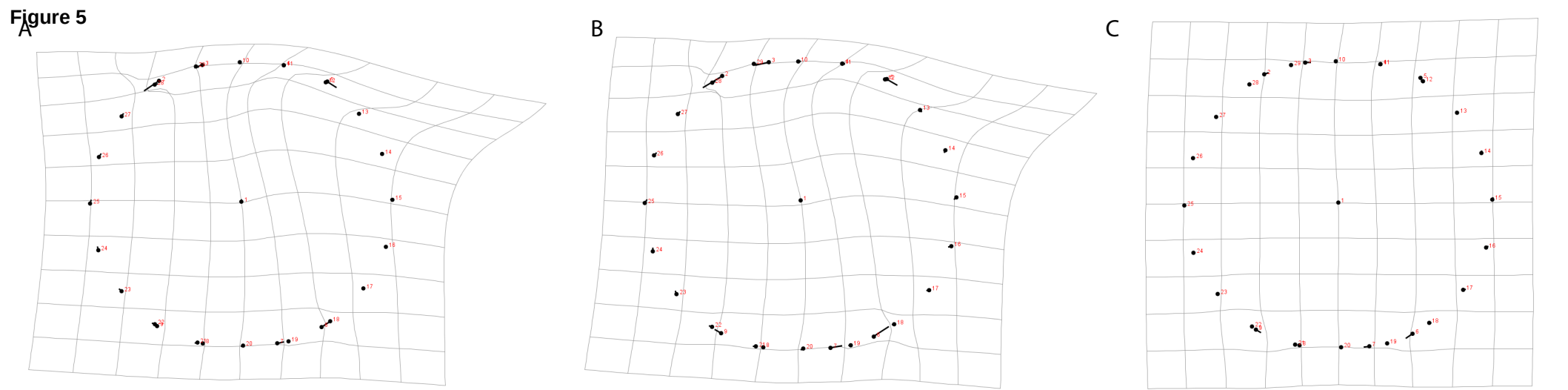

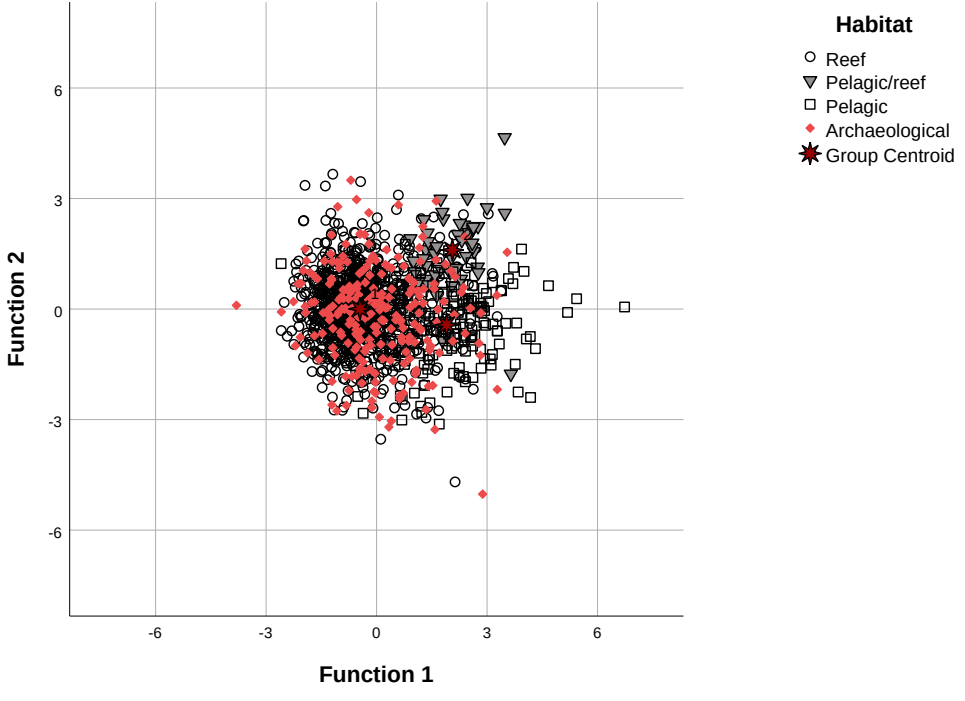
Habitat
Reef
Pelagic/reef
Pelagic
Archaeological
Group Centroid
Function 2
Function 1
6
3
0
-3
-6
-6
-3
0
3
6

Precaudal all families and archaeological

Click here to download Raw research data (under CC BY license; see above): Precaudal all families and archaeological.dat

Caudal all families and archaeological

Click here to download Raw research data (under CC BY license; see above): Caudal all families and archaeological.dat